

# The *Arabidopsis* LUT1 locus encodes a member of the cytochrome P450 family that is required for carotenoid $\epsilon$ -ring hydroxylation activity

Li Tian, Valeria Musetti, Joonyul Kim, Maria Magallanes-Lundback, and Dean DellaPenna\*

Department of Biochemistry and Molecular Biology, Michigan State University, East Lansing, MI 48824

Communicated by Jan A. D. Zeevaart, Michigan State University, East Lansing, MI, November 6, 2003 (received for review October 2, 2003)

Lutein, a dihydroxy xanthophyll, is the most abundant carotenoid in plant photosynthetic tissues and plays crucial structural and functional roles in the light-harvesting complexes. Carotenoid  $\beta$ - and  $\epsilon$ -hydroxylases catalyze the formation of lutein from  $\alpha$ -carotene ( $\beta, \epsilon$ -carotene). In contrast to the well studied  $\beta$ -hydroxylases that have been cloned and characterized from many organisms, the  $\epsilon$ -hydroxylase has only been genetically defined by the *lut1* mutation in *Arabidopsis*. We have isolated the *LUT1* gene by positional cloning and found that, in contrast to all known carotenoid hydroxylases, which are the nonheme diiron monooxygenases, *LUT1* encodes a cytochrome P450-type monooxygenase, CYP97C1. Introduction of a null mutant allele of *LUT1*, *lut1-3*, into the  $\beta$ -hydroxylase 1/ $\beta$ -hydroxylase 2 (*b1 b2*) double-mutant background, in which both *Arabidopsis*  $\beta$ -hydroxylases are disrupted, yielded a genotype (*lut1-3 b1 b2*) in which all three known carotenoid hydroxylase activities are eliminated. Surprisingly, hydroxylated  $\beta$ -rings were still produced in *lut1-3 b1 b2*, suggesting that a fourth unknown carotenoid  $\beta$ -hydroxylase exists *in vivo* that is structurally unrelated to  $\beta$ -hydroxylase 1 or 2. A second chloroplast-targeted member of the CYP97 family, CYP97A3, is 49% identical to *LUT1* and hypothesized as a likely candidate for this additional  $\beta$ -ring hydroxylation activity. Overall, *LUT1* defines a class of carotenoid hydroxylases that has evolved independently from and uses a different mechanism than nonheme diiron  $\beta$ -hydroxylases.

Carotenoids are terpenoid compounds that perform a variety of critical roles in photosystem structure, light harvesting, and photoprotection. Lutein (3*R*,3'*R*- $\beta, \epsilon$ -carotene-3,3'-diol), is the most abundant carotenoid in all plant photosynthetic tissues, in which it plays an important role in light-harvesting complex II assembly and function. Zeaxanthin (3*R*,3'*R*- $\beta, \beta$ -carotene-3,3'-diol) is a structural isomer of lutein and is a critical component of nonphotochemical quenching (1, 2). The synthesis of lutein and zeaxanthin involves cyclization of lycopene to form  $\alpha$ - and  $\beta$ -carotene, respectively, followed by the introduction of hydroxyl groups onto the ionone rings by a class of enzymes known as carotenoid hydroxylases (Fig. 1).  $\beta$ -Hydroxylases add hydroxyl groups to carbon 3 (C-3) of  $\beta$ -rings, whereas hydroxylation of C-3 on  $\epsilon$ -rings is carried out by  $\epsilon$ -hydroxylases. Two  $\beta$ -ring hydroxylations of  $\beta$ -carotene yield zeaxanthin, whereas one  $\beta$ -ring and one  $\epsilon$ -ring hydroxylation of  $\alpha$ -carotene yield lutein (Fig. 1).

Based on the stereospecific introduction of C-3 hydroxyl groups and the requirement for molecular oxygen, carotenoid hydroxylation reactions were predicted to be catalyzed by mixed-function oxygenases such as the cytochrome P450 enzymes (3–5). However,  $\beta$ -hydroxylases have been cloned from a variety of photosynthetic and nonphotosynthetic bacteria, green algae, and plants (6) and in all three phyla encode nonheme diiron proteins that have a fundamentally different hydroxylation reaction mechanism than heme-binding cytochrome P450 enzymes (7). Biochemical analysis and mutagenesis of pepper (*Capsicum annuum*)  $\beta$ -hydroxylases have confirmed that the enzymes require iron, ferredoxin, and ferredoxin oxidoreductase for activity and that all 10 of the conserved iron-coordinating histidines are

required for activity (8). The *Arabidopsis* genome encodes two nonheme diiron  $\beta$ -hydroxylases ( $\beta$ -hydroxylases 1 and 2), and although both efficiently hydroxylate  $\beta$ -rings, they function poorly with  $\epsilon$ -ring-containing substrates *in vitro* (9, 10).

Early isotope-labeling studies have shown that carotenoid hydroxylation reactions are stereospecific (3, 4). The chirality of the hydroxylated  $\epsilon$ -ring C-3 is opposite to that of the hydroxylated  $\beta$ -ring C-3. This difference in product chirality was an initial suggestion that two distinct hydroxylases are needed for  $\beta$ - and  $\epsilon$ -ring hydroxylations and may partially explain why  $\beta$ -hydroxylases function poorly with  $\epsilon$ -ring-containing substrates *in vitro*. Mutational studies in *Arabidopsis* have provided genetic evidence for the existence of a distinct  $\epsilon$ -ring-specific hydroxylase (11). Mutation of the *LUT1* locus in *Arabidopsis* decreased the production of lutein by 80–95% (dependent on plant age) and resulted in accumulation of the monohydroxy precursor zeinoxanthin, a classic phenotype for a mutation affecting a biosynthetic enzyme.  $\epsilon$ -Ring hydroxylation was specifically blocked in *lut1*, and production of  $\beta$ -carotene-derived xanthophylls was increased. From these data, it was proposed that *LUT1* encodes a function specific for  $\epsilon$ -ring hydroxylation (11).

The interactions and functional redundancies of the three known carotenoid hydroxylases in *Arabidopsis* ( $\beta$ -hydroxylases 1 and 2 and *LUT1*) have been studied *in vivo* by isolating mutations disrupting each gene and generating multiple hydroxylase-deficient mutant genotypes (12). In the  $\beta$ -hydroxylase 1/ $\beta$ -hydroxylase 2 double-null mutant (*b1 b2*), in which both known  $\beta$ -hydroxylases were eliminated, hydroxylated  $\beta$ -ring groups were still synthesized at significant levels (75% of wild type), indicating that an additional  $\beta$ -ring hydroxylation activity exists *in vivo*. The ethyl methane sulfonate (EMS)-derived *lut1-2* mutation was introduced into the *b1 b2* background to address whether this additional  $\beta$ -hydroxylase activity might be a secondary function of the  $\epsilon$ -hydroxylase or be due to a third unrelated  $\beta$ -hydroxylase. Hydroxylated  $\beta$ -ring groups were reduced further to 60% of wild-type levels in the *lut1-2 b1 b2* triple mutant (12), suggesting that *LUT1* is capable of  $\beta$ -ring hydroxylation *in vivo*. However, a caveat of this experiment is that *LUT1* activity may not have been completely eliminated in the EMS-derived *lut1-2* mutant, and we could not resolve whether the remaining  $\beta$ -ring hydroxylation in *lut1-2 b1 b2* was caused by residual *LUT1* activity or the presence of a third unrelated  $\beta$ -hydroxylase. Cloning of the *LUT1* locus and generation of a null  $\epsilon$ -hydroxylase mutant are required to further understanding of *in vivo* carotenoid hydroxylase activity and for applying molecular genetic approaches to study carotenoid hydroxylase functions *in vivo*.

Abbreviations: EMS, ethyl methane sulfonate; T-DNA, portion of the tumor-inducing plasmid that is transferred to plant cells.

Data deposition: The cDNA sequence reported in this paper has been deposited in the GenBank database (accession no. AY424805).

\*To whom correspondence should be addressed. E-mail: dellapenna@msu.edu.

© 2004 by The National Academy of Sciences of the USA

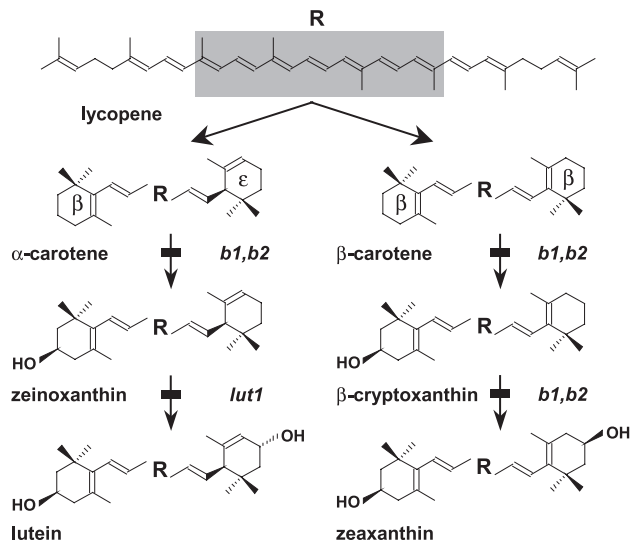


**Fig. 1.** Biosynthetic steps leading to lutein and zeaxanthin from lycopene. Carotenoid ring hydroxylations are key reactions for the biosynthesis of lutein and zeaxanthin. The steps blocked by the *b1* ( $\beta$ -hydroxylase 1), *b2* ( $\beta$ -hydroxylase 2), and *lut1* ( $\epsilon$ -hydroxylase) mutations are indicated.

Prior attempts to clone an  $\epsilon$ -ring-specific hydroxylase by sequence-based similarity to  $\beta$ -hydroxylases in *Arabidopsis* were not successful and only identified the  $\beta$ -hydroxylase 2 gene (10). A thorough search of the fully sequenced *Arabidopsis* genome also failed to identify any additional genes bearing significant similarity to  $\beta$ -hydroxylases from plants, cyanobacteria, and nonphotosynthetic bacteria (10). These results suggested that the  $\epsilon$ -hydroxylase defines a structurally distinct carotenoid hydroxylase family. We report here identification of the *LUT1* locus by positional cloning and show that *LUT1* indeed defines a previously uncharacterized class of carotenoid hydroxylases in nature.

## Materials and Methods

**Positional Cloning of *LUT1*.** Homozygous *lut1-1* (ecotype Columbia) was crossed to wild-type *Landsberg erecta*.  $F_2$  progeny homozygous for the *lut1* mutation were identified by a TLC screening method. Briefly, carotenoid samples were extracted as described (10), resuspended in ethyl acetate, spotted on a silica TLC plate (J. T. Baker), and developed in 90:10 (v/v) hexane/isopropanol.  $F_2$  plants homozygous for *lut1* contain a characteristic extra yellow band caused by accumulation of zeinoxanthin.

Genomic DNA from homozygous *lut1*  $F_2$  plants was isolated by using the DNAzol reagent following manufacturer instructions (Invitrogen). PCRs were performed with 1  $\mu$ l of genomic DNA in a 20- $\mu$ l reaction mixture. The PCR program was 94°C for 3 min, 60 cycles of 94°C for 15 s, 50–60°C (the annealing temperature was optimized for each specific pair of primers) for 30 s, 72°C for 30 s, and finally 72°C for 10 min. A portion of the PCR product then was separated on a 3% agarose gel. *lut1* had been mapped previously to 67  $\pm$  3 centimorgans on chromosome 3 (10). Additional simple sequence length polymorphism markers for fine-mapping in this interval were designed based on the insertions/deletions information obtained from the Monsanto web site ([www.arabidopsis.org/Cereon](http://www.arabidopsis.org/Cereon)).

**Cosmid Screening and Complementation of *lut1*.** An *Arabidopsis* cosmid library (13) was screened, and cosmids carrying the *At3g53130* gene were identified. For complementation of the *lut1* mutation, a 4.2-kb restriction fragment containing the *At3g53130* gene was subcloned into the pMLBART vector (14). Homozygous *lut1* plants were transformed with *Agrobacterium tumefaciens*

strain GV3101 containing pMLBART-*At3g53130* by using the floral dip method (15). Basta-resistant  $T_1$  transformants were selected, and the carotenoid composition of leaf tissue was analyzed by HPLC (10).

**Isolation of T-DNA Knockout Mutants in *At3g53130* and Generation of a Carotenoid Hydroxylase Triple-Knockout Mutant Line.** *At3g53130*-specific primers (forward, 5'-CTTCCTCTTCTTACTCT-TCTCTCTTCACT-3'; reverse, 5'-AAGAACGATGGATGT-TATAGACTGAAATC-3') were sent to the University of Wisconsin *Arabidopsis* T-DNA (portion of the tumor-inducing plasmid that is transferred to plant cells) knockout facility to identify knockout mutants of the *LUT1* gene. A single knockout line, designated *lut1-3*, was identified and isolated as described ([www.biotech.wisc.edu/Arabidopsis](http://www.biotech.wisc.edu/Arabidopsis)). To generate a hydroxylase triple-knockout mutant line, homozygous *lut1-3* and *b1 b2* plants were crossed. Putative *lut1-3 b1 b2* triple mutants were identified from the segregating  $F_2$  population by HPLC, and their genotypes were confirmed by PCR as described (12).

**TaqMan Real-Time PCR Assay.** *LUT1* mRNA levels were quantified by TaqMan real-time PCR by using elongation factor 1 $\alpha$  mRNA levels for normalization (12). The *LUT1* TaqMan probe and primers are: 5'-CCGTCTCGCTGCTGGTCTCG-3' (TaqMan probe), 5'-GGATGAATGAGTACGGACCCAT-3' (forward primer), and 5'-GGGTCGCTCACAATTACGAAA-3' (reverse primer). The relative quantity of the transcripts was calculated by using the comparative threshold cycle ( $C_T$ ) method (16).

**Phylogenetic Analysis of *LUT1* Homologs.** Full-length protein sequences of putative *LUT1* homologs from *Arabidopsis thaliana*, *Glycine max*, *Oryza sativa*, and *Pisum sativum* were obtained from GenBank: CYP97A3 (accession no. AAL08302), CYP97B1 (accession no. CAA89260), CYP97B2 (accession no. AAB94586), CYP97B3 (accession no. CAB10290), CYP97C1 (accession no. AAM13903), CYP97C2 (accession no. AAK20054), and CYP86A8 (accession no. CAC47665). Rice CYP97A4 and CYP97B4 sequences were obtained from the cytochrome P450 web site (<http://drnelson.utmem.edu/CytochromeP450.html>).

Additional plant *LUT1* homologs were retrieved from The Institute of Genome Research Unique Gene Indices: TC76166 (*Hordeum vulgare*), TC163981 (*G. max*), and TC69886 (*H. vulgare*). The coding sequences of each were extracted, assembled, and corrected by the ESTSCAN program (<http://tigrblast.tigr.org/tgi>). Chlamydomonas CYP97A3 homolog (Scaffold1399) was obtained from the Department of Energy Joint Genome Institute (JGI) database (<http://genome.jgi-psf.org/chlre1/chlre1.home.html>). Truncated *LUT1* homologs from *Zea mays*, lettuce, and cotton are also present in the databases but were not used for phylogenetic analysis because full-length assemblies were not possible.

The deduced amino acid sequences of *LUT1* homologs were aligned by using the CLUSTALX algorithm (17). A neighbor-joining (18) tree was constructed based on the sequence alignment and tested further with 500 bootstrap resamplings by using the computer program MEGA2 2.1 (19). Poisson-correction distance was used with 340 amino acids after removing gaps.

## Results

**Fine-Mapping of the *LUT1* Locus.** The *LUT1* locus has been mapped to the bottom arm of chromosome 3 at 67  $\pm$  3 centimorgans (10). For fine-mapping of the locus, 530 plants homozygous for the *lut1* mutation were identified from  $\approx$ 2,000 plants in a segregating  $F_2$  mapping population. By using simple sequence length polymorphism markers, *LUT1* was initially localized to an interval spanning two bacterial artificial chromosome clones (F8J2 and T4D2) and was delineated further to a 100-kb interval

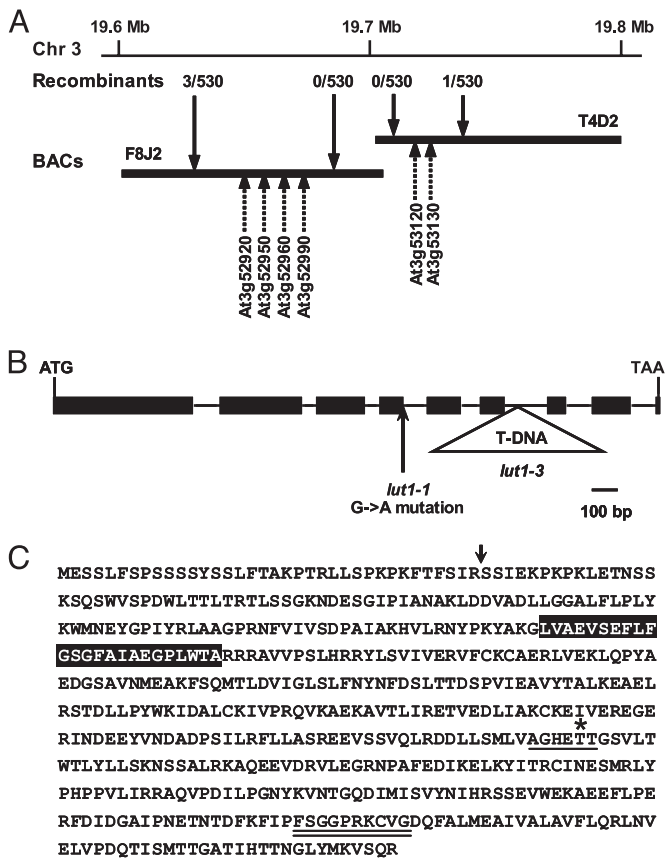


**Fig. 2.** Positional cloning of the *LUT1* locus. (A) Fine-mapping of the interval containing *LUT1*. Recombinants are indicated for specific simple sequence length polymorphism markers across the interval, and the position of chloroplast-targeted proteins are indicated by dashed arrows. BACs, bacterial artificial chromosomes. (B) Overview of the intron–exon organization of *LUT1* and the locations of the *lut1-1* and *lut1-3* mutations. (C) Deduced amino acid sequence of *LUT1*. The cleavage site of the putative chloroplast-targeting sequence is indicated by an arrow, and the single predicted transmembrane domain is shaded in black. The conserved cytochrome P450 molecular oxygen-binding pocket and the cysteine motif are indicated by single and double underlines, respectively, and the conserved Thr is indicated by an asterisk.

containing 30 predicted proteins (Fig. 2A). As with all other carotenoid biosynthetic enzymes, the *LUT1* gene product is predicted to be chloroplast-targeted, and within the 100-kb interval containing *LUT1*, six proteins were predicted as being chloroplast-targeted by TARGETP prediction software (www.cbs.dtu.dk/services/TargetP). One of these chloroplast-targeted proteins, At3g53130, is a member of the cytochrome P450 monooxygenase family (CYP97C1). Cytochrome P450 monooxygenases are heme-binding proteins that insert a single oxygen atom into substrates (e.g., hydroxylation reactions), and therefore At3g53130 was considered to be a strong candidate for *LUT1*.

**Mutant Complementation, Characterization, and the Identification of *LUT1*.** The identity of At3g53130 as *LUT1* was initially demonstrated by molecular complementation analysis. Homozygous *lut1-1* mutants were transformed with a 4.2-kb genomic DNA fragment from wild-type Columbia (the background of *lut1*) containing the At3g53130 coding region, 1.0 kb upstream of the start codon and 0.7 kb downstream of the stop codon. Eight independent transformants were selected, and all showed a wild-type lutein level when analyzed by HPLC (Fig. 3D). These

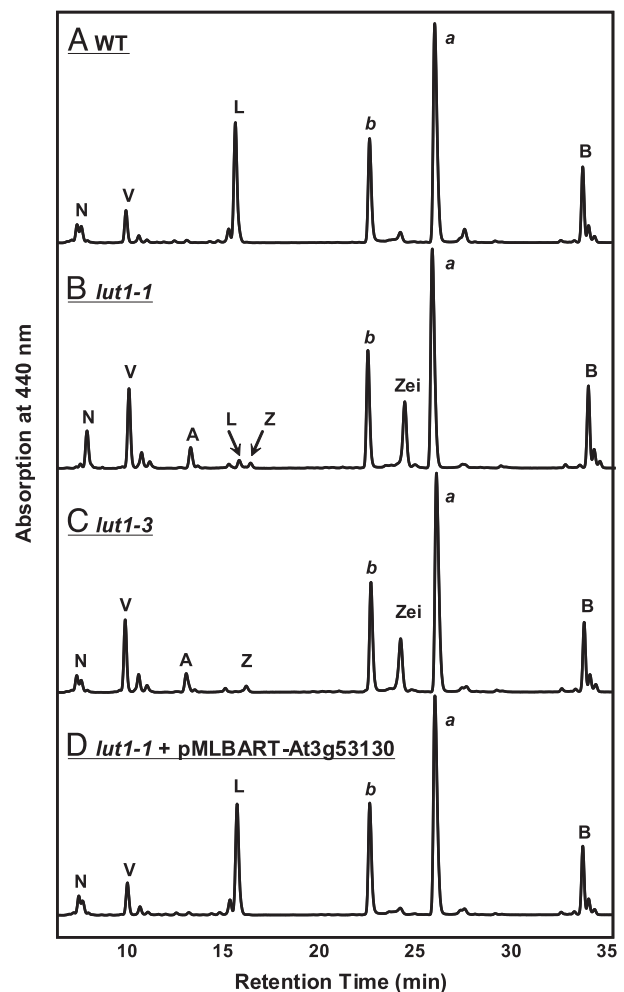


**Fig. 3.** HPLC elution profiles of total leaf carotenoid extracts from wild type (A), *lut1-1* (B), *lut1-3* (C), and *lut1-1* transformed with pMLBART-At3g53130 (D). Peaks correspond to neoxanthin (N), violaxanthin (V), antheraxanthin (A), lutein (L), zeaxanthin (Z), chlorophyll *b* (*b*), zeinoxanthin (Zei), chlorophyll *a* (*a*), and  $\beta$ -carotene (B).

data indicate that At3g53130 genomic DNA can complement the *lut1* mutation.

To determine the molecular basis of the *lut1* mutations, we sequenced both original EMS-derived *lut1* alleles (11). The *lut1-1* allele contains a G-to-A mutation at the highly conserved exon/intron splice junction (5'-AG/GT; the mutated G is in bold) that would cause an error in RNA splicing and lead to production of a mistranslated protein (Fig. 2B). The coding region of the *lut1-2* allele was sequenced fully, but no mutations were identified. However, a rearrangement in the upstream region of the *lut1-2* allele was identified by Southern blot analysis but was not characterized further (data not shown). A third *lut1* allele, *lut1-3*, was identified by screening a T-DNA knockout population by using At3g53130-specific primers. *Lut1-3* contains a T-DNA insertion in the sixth intron of the *LUT1* gene (Fig. 2B).

To compare the impact of different *lut1* alleles on carotenoid composition, total carotenoids were extracted from 4-week-old wild-type, *lut1-1*, *lut1-2* (data not shown), and *lut1-3* plants and separated by HPLC (Fig. 3A–C). *Lut1-1* and *lut1-2* accumulated the monohydroxy biosynthetic intermediate zeinoxanthin and contained 8% of wild-type lutein, consistent with prior report (11). In contrast, although *lut1-3* also accumulated zeinoxanthin, it lacked lutein (Fig. 3C), indicating that  $\epsilon$ -ring hydroxylation

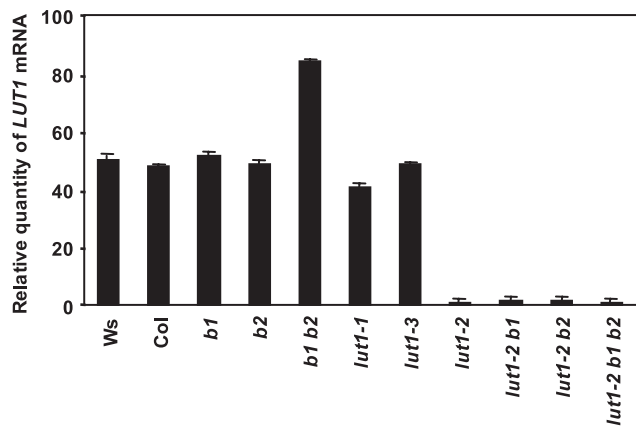


**Fig. 4.** The relative wild-type or mutant *LUT1* transcript level detected in each genotype by real-time PCR (refer to *Materials and Methods*). The relative quantity of the *LUT1* mRNA has been corrected with elongation factor 1 $\alpha$ . Data shown are means with SD ( $n = 6$ ). Ws, Wassilewskija; Col, Columbia.

function is eliminated by disruption of the *At3g53130* gene. The *lut1-3* phenotype also indicates that redundant  $\epsilon$ -ring hydroxylation activities are not present in leaves and that the previously reported EMS-mutagenized *lut1-1* and *lut1-2* alleles are indeed leaky for  $\epsilon$ -ring hydroxylation activity (11) (Fig. 3B). Taken together, the complementation of the *lut1-1* mutation with a wild-type *At3g53130* gene, the point mutation at a conserved splice site in the *lut1-1* allele, and the phenotype of the *At3g53130* T-DNA knockout mutant conclusively demonstrate that *At3g53130* is the *LUT1* locus.

**LUT1 Encodes a Chloroplast-Targeted Cytochrome P450 with a Single Transmembrane Domain.** The deduced amino acid sequence of LUT1 contains several features characteristic of cytochrome P450 enzymes (Fig. 2C). Cytochrome P450 monooxygenases contain a consensus sequence of (A/G)GX(D/E)T(T/S) that forms a binding pocket for molecular oxygen with the invariant Thr residue playing a critical role in oxygen binding in both prokaryotic and eukaryotic cytochrome P450s (20). In the deduced LUT1 protein sequence, this oxygen-binding pocket is highly conserved (Fig. 2C, single-underlined amino acids). The conserved sequence around the heme-binding cysteine residue for cytochrome P450-type enzymes is FXXGXXXCXG and is also present in LUT1 (Fig. 2C, double-underlined amino acids).

The chloroplast transit peptide prediction software CHLOROP 1.1 ([www.cbs.dtu.dk/services/ChloroP](http://www.cbs.dtu.dk/services/ChloroP)) predicts an N-terminal transit peptide in LUT1 that is cleaved between Arg-36 and Ser-37 (Fig. 2C). The predicted chloroplast localization for LUT1 is consistent with the subcellular localization of carotenoid biosynthesis in higher plants (6) but is uncommon for a plant cytochrome P450. Of the 272 predicted cytochrome P450s in the *Arabidopsis* genome, only nine, including LUT1, are predicted to be chloroplast-targeted (21). LUT1 also contains a single predicted transmembrane domain (Fig. 2C, shaded box), which contrasts with the four transmembrane domains predicted for the nonheme diiron  $\beta$ -hydroxylases (6). Initial attempts to express and assay LUT1 protein in yeast were unsuccessful.

**LUT1 Gene Expression and *in Vivo* Activity in the  $\beta$ -Hydroxylase-Deficient Backgrounds.** Characterization of previously isolated T-DNA knockouts in the two *Arabidopsis*  $\beta$ -hydroxylase genes suggested that  $\beta$ - and  $\epsilon$ -hydroxylases have overlapping functions *in vivo* (12). To investigate whether  $\epsilon$ -hydroxylase expression is affected in the various carotenoid hydroxylase mutant backgrounds, steady-state *LUT1* mRNA levels were quantified by real-time PCR (Fig. 4). The *LUT1* TaqMan probe hybridizes 336

**Table 1.  $\beta$ -Xanthophyll production and  $\beta$ -ring hydroxylation in leaf tissue of wild-type and carotenoid hydroxylase mutants**

Genotype	$\beta$ -Xanthophylls*	Hydroxylated $\beta$ -rings <sup>†</sup>
Ws	54.0 $\pm$ 2.7 <sup>a†</sup>	48.5 $\pm$ 1.0 <sup>a</sup>
Col	60.7 $\pm$ 7.6 <sup>a</sup>	48.7 $\pm$ 0.9 <sup>a</sup>
<i>b1 b2</i>	20.5 $\pm$ 4.8 <sup>b</sup>	40.2 $\pm$ 1.4 <sup>b</sup>
<i>lut1-2 b1 b2</i>	26.5 $\pm$ 3.4 <sup>b</sup>	33.6 $\pm$ 2.4 <sup>c</sup>
<i>lut1-3 b1 b2</i>	28.3 $\pm$ 4.6 <sup>b</sup>	31.1 $\pm$ 1.2 <sup>c</sup>

Total carotenoids were extracted from 5-week-old plants and quantified by HPLC as described (12).

\* $\beta$ -Xanthophylls are the sum of zeaxanthin, antheraxanthin, violaxanthin, and neoxanthin as mmol of pigment/mol of chlorophyll *a* + *b*.

<sup>†</sup>Data are given as percentage of total ring hydroxylation.

<sup>‡</sup>All values are means  $\pm$  SD ( $n = 6$ ). Values marked with the same letters are not significantly different from each other within a column (Student's *t* test,  $P > 0.05$ ).

bp downstream from the start codon. *LUT1* mRNA levels are not significantly different from wild type in the  $\beta$ -hydroxylase single mutants (*b1* and *b2*) but are increased significantly in the  $\beta$ -hydroxylase double mutant *b1 b2* (Fig. 4). *LUT1* mRNA levels in *lut1-2* alone and in combination with various  $\beta$ -hydroxylase mutant loci (i.e., *lut1-2 b1*, *lut1-2 b2*, and *lut1-2 b1 b2*) are similar and reduced to 2% of wild-type levels, consistent with the rearrangement of the upstream region in *lut1-2* negatively impacting *LUT1* transcription. The steady-state levels of modified *LUT1* transcript in *lut1-1* and *lut1-3* are similar to wild-type transcript levels suggesting that, although LUT1 activity is negatively impacted in each mutant, *LUT1* transcription is not.

The phenotype of the previously isolated *lut1-2 b1 b2* mutant was not conclusive because of the leaky nature of the EMS-derived *lut1-2* allele. Cloning of *LUT1* and isolation of the *LUT1* knockout mutant, *lut1-3*, allow for the complete elimination of LUT1 activity *in vivo*. *Lut1-3* was crossed to *b1 b2*, and homozygous *lut1-3 b1 b2* mutants were isolated. There was no lutein production in the *lut1-3 b1 b2* triple mutant (data not shown), consistent with the *lut1-3* single mutant phenotype (Fig. 3C). The total moles of  $\beta$ -carotene-derived xanthophylls produced are not significantly different between *lut1-2 b1 b2* and *lut1-3 b1 b2* (Table 1). However, when one considers the total moles of hydroxylated  $\beta$ -rings produced in each mutant (which includes hydroxylated  $\beta$ -ring in zeinoxanthin), total hydroxylated  $\beta$ -rings are reduced significantly in *lut1-2 b1 b2* and *lut1-3 b1 b2* compared to *b1 b2*, suggesting that LUT1 also has  $\beta$ -ring hydroxylation activity *in vivo* (Table 1). In addition, the presence of  $\beta$ -carotene-derived xanthophylls in the triple-knockout mutant *lut1-3 b1 b2* indicates that a third  $\beta$ -hydroxylase must exist *in vivo* (Table 1).

**CYP97 Homologs in Other Species.** *Arabidopsis* LUT1 was designated previously as CYP97C1 according to the standardized cytochrome P450 nomenclature ([www.biobase.dk/P450](http://www.biobase.dk/P450)). The *Arabidopsis* genome also contains two other CYP97 family members, CYP97A3 and CYP97B3, which are 49% and 42% identical to the LUT1 protein, respectively. Interestingly, CYP97A3 (At1g31800) is also one of the nine cytochrome P450s in *Arabidopsis* predicted to be chloroplast-targeted, whereas CYP97B3 (At4g15110) is predicted to be targeted to the mitochondria (21). Additional CYP97 family proteins were identified in the EST and genomic databases from a wide variety of monocots and dicots including *Arabidopsis*, barley, rice, soybean, and pea (Fig. 5).

## Discussion

Several independent lines of evidence confirm that the *Arabidopsis*  $\epsilon$ -hydroxylase/*LUT1* locus is a cytochrome P450 mono-

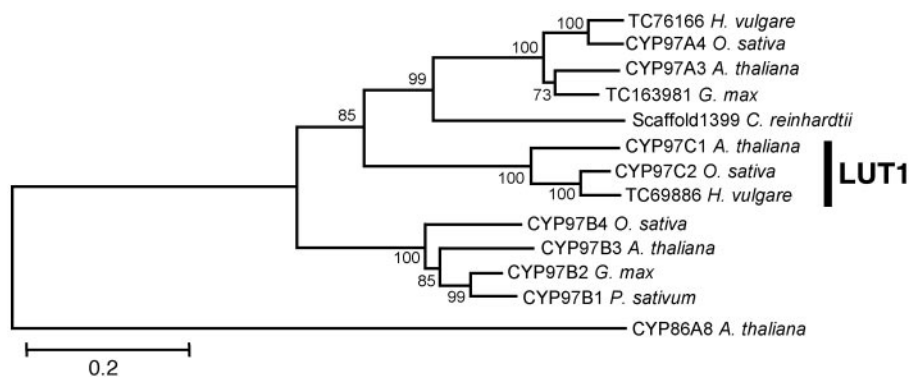


**Fig. 5.** Phylogenetic analysis of LUT1. A rooted neighbor-joining tree was constructed by using the fatty acid  $\omega$ -hydroxylase (CYP86A8) from *A. thaliana* as an outgroup. Bootstrap values are indicated adjacent to the branches. Accession numbers for the sequences used are listed in *Materials and Methods*.

oxygenase, encoded by At3g53130. The cytochrome P450  $\epsilon$ -hydroxylase carries out a type of hydroxylation reaction that is mechanistically distinct from the nonheme diiron  $\beta$ -hydroxylases and has evolved independently of the  $\beta$ -hydroxylases. The absence of lutein in the *LUT1*-null knockout allele, *lut1-3*, demonstrates that LUT1 is the only  $\epsilon$ -hydroxylase activity in photosynthetic tissues. Thus, although  $\beta$ -hydroxylases have been shown to use  $\epsilon$ -ring substrates *in vitro* with low efficiency (9, 10), they do not contribute to  $\epsilon$ -ring hydroxylation activity *in vivo* and cannot compensate for the lack of  $\epsilon$ -ring hydroxylation activity in *lut1-3*.

**Isolation of a Hydroxylase Triple-Knockout Mutant Indicates the Existence of a Third, Previously Uncharacterized  $\beta$ -Hydroxylase *in Vivo*.** Previous work with mutant genotypes defective in one or more of the carotenoid hydroxylases ( $\beta$ -hydroxylases 1 and 2 and LUT1) suggested that LUT1 may be active toward  $\beta$ -rings (12). The *b1 b2* double mutant lacks both known  $\beta$ -hydroxylases, but the level of hydroxylated  $\beta$ -rings is only reduced 25% relative to wild type, indicating that other  $\beta$ -ring hydroxylation activity must exist. The introduction of the *lut1-2* allele (now known to be a leaky mutation) into the *b1 b2* background led to an additional 15% reduction of hydroxylated  $\beta$ -rings relative to wild type, consistent with LUT1 contributing to  $\beta$ -ring hydroxylation *in vivo*. Induction of *LUT1* expression in the *b1 b2* double mutant is also consistent with the hypothesis that the  $\beta$ -ring hydroxylation deficiency in *b1 b2* is partially compensated by up-regulating expression of the *LUT1* gene (Fig. 4).

To test whether LUT1 is the only additional  $\beta$ -ring hydroxylation activity in the *b1 b2* background, the *LUT1*-null allele, *lut1-3*, was introduced into the *b1 b2* double-mutant background. Were LUT1 the only additional  $\beta$ -ring hydroxylation activity *in vivo*, the *lut1-3 b1 b2* triple mutant would lack all xanthophylls and likely be lethal. However, hydroxylated  $\beta$ -ring groups are still produced in *lut1-3 b1 b2* at levels similar to *lut1-2 b1 b2* (Table 1), which clearly indicates that a fourth unknown carotenoid hydroxylation activity exists that is specific for  $\beta$ -rings *in vivo*. This activity is not a nonheme diiron  $\beta$ -hydroxylase, because no additional nonheme diiron  $\beta$ -hydroxylase homologs are present in the *Arabidopsis* genome (10). Phylogenetic analysis of LUT1 homologs reveals that the closest homolog in *Arabidopsis*, CYP97A3 (Fig. 5), is also chloroplast-targeted. CYP97A3 does not have  $\epsilon$ -ring hydroxylation activity based on the *lut1-3* phenotype (Fig. 2C) but is a likely candidate for the additional  $\beta$ -hydroxylase in the *lut1-3 b1 b2* triple mutant.

**$\beta$ - and  $\epsilon$ -Ring Hydroxylases Have Different Hydroxylation Mechanisms.** Carotenoid  $\beta$ - and  $\epsilon$ -hydroxylases add hydroxyl groups to the  $\beta$ - and  $\epsilon$ -rings of carotenes, respectively.  $\beta$ - and  $\epsilon$ -rings are

quite similar in structure and differ only in the placement of a double bond on the ring structure (Figs. 1 and 6). In a  $\beta$ -ring this double bond is conjugated with the polyene chain, whereas in an  $\epsilon$ -ring it is not, and hence the relative conformations of the two rings to the polyene chain differ. Given the degree of similarity of the two substrates, why would two different types of monooxygenases be required for carotene hydroxylation reactions in *Arabidopsis*?

Hydroxylation of both  $\beta$ - and  $\epsilon$ -rings requires the abstraction of a hydrogen atom from the C-3 position of each ring (Fig. 6A). However, it is energetically more favorable to withdraw a C-3 hydrogen atom from an  $\epsilon$ -ring than from a  $\beta$ -ring (dissociation energy 86 kcal/mol vs. 100 kcal/mol, respectively) (22). This is because the  $\epsilon$ -ring C-3 is an allylic carbon and produces a resonance-stabilized allylic radical after hydrogen abstraction, whereas the nonallylic  $\beta$ -ring C-3 cannot (Fig. 6A). This suggests that  $\beta$ -rings may require a stronger oxidant for hydrogen ab-

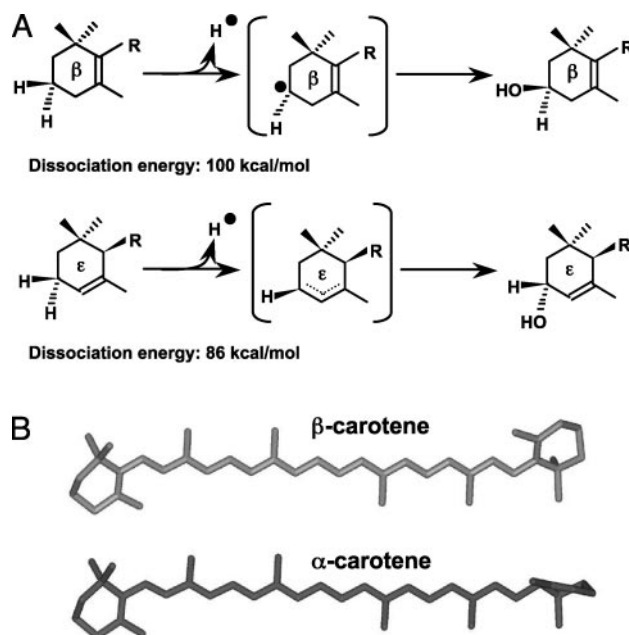


**Fig. 6.** The substrates and proposed mechanisms of carotenoid hydroxylation reactions. (A) The hydroxylation reactions of  $\beta$ - and  $\epsilon$ -rings. R, polyene chain. (B) Three-dimensional structures of  $\alpha$ - and  $\beta$ -carotene hydroxylation substrates. The left rings of both molecules are  $\beta$ -rings, and the right rings are  $\beta$ - and  $\epsilon$ -rings, respectively, for  $\beta$ - and  $\alpha$ -carotene.

straction, raising the possibility that the nonheme diiron  $\beta$ -hydroxylase is a stronger oxidant than the cytochrome P450  $\epsilon$ -hydroxylase.

Both cytochrome P450-type and nonheme diiron-type monooxygenases hydroxylate substrates by a hydrogen atom-abstraction/oxygen-rebound mechanism with a short-lived iron-oxo intermediate. The key cytochrome P450 intermediate is an  $\text{Fe}^{\text{IV}}=\text{O}$  porphyrin  $\pi$ -radical cation (23), whereas the key nonheme diiron monooxygenase intermediate is a di- $\text{Fe}^{\text{IV}}$  unit with bridging oxos (24). Experimental evidence has shown that both types of enzymes are able to add oxygen to allylic and nonallylic C—H bonds (25, 26), and hence both  $\beta$ - and  $\epsilon$ -hydroxylases can produce oxidants sufficient to extract a hydrogen atom from both types of rings. Therefore, the requirement of two fundamentally different types of hydroxylases for  $\beta$ - and  $\epsilon$ -rings cannot simply be explained by their oxidation capacities relative to their different substrates.

Another key factor that determines enzyme catalysis is the access to and binding of substrates. Neither the  $\beta$ - nor the  $\epsilon$ -hydroxylase has been crystallized; therefore the precise conformations of their substrate-binding sites are not known. However, small differences in the carotenoid ring structures may contribute to the different substrate specificity of the enzymes.  $\beta$ -Rings have a double bond in conjugation with the polyene chain and hence are restrained to the same plane as the polyene chain, whereas the double bond of  $\epsilon$ -rings is not in conjugation and has relatively free rotation around the C6'–C7' carbon (Fig. 6B). One possible explanation for the differing hydroxylase substrate specificity is that the substrate-binding pocket of  $\beta$ -hydroxylases can only accommodate a straight-chain hydrocarbon (e.g.,  $\beta$ -rings) and not a ring that is tilted from the polyene chain (e.g.,  $\epsilon$ -rings). The opposite could be true of substrate binding by the  $\epsilon$ -hydroxylase. Another possible explanation is that although both hydroxylases may bind  $\beta$ - and  $\epsilon$ -ring substrates, only one of the ring structures is in the correct orientation for efficient C-3 hydrogen atom abstraction and subsequent oxidation by the respective enzyme. Therefore, it is likely that the stereochemistry of substrates leads to the specificity of each hydroxylase enzyme.

**Evolution of the  $\epsilon$ -Hydroxylase.** The identification of the *LUTI* locus as a cytochrome P450 enzyme makes it clear that the  $\epsilon$ -hydroxylases evolved independently of  $\beta$ -hydroxylases, which have invariably been shown to be nonheme diiron enzymes (10). Putative  $\epsilon$ -hydroxylase homologs have been identified in mono-

cot (e.g., rice) and dicot (e.g., soybean and pea) databases, suggesting that the enzyme is widespread in the plant kingdom. The obvious question becomes: What is the evolutionary origin of the  $\epsilon$ -hydroxylase in plants?

Although the exact driving force for the evolution of the  $\epsilon$ -hydroxylase is unknown, it may have evolved in parallel with the evolution of its substrate,  $\alpha$ -carotene ( $\beta,\epsilon$ -carotene). The  $\epsilon$ -hydroxylase product, lutein, has only been identified in land plants and the green algae that gave rise to land plants (27). Although cyanobacteria do not contain lutein, the biosynthetic precursor of lutein,  $\alpha$ -carotene, is present in two cyanobacteria: *Prochlorococcus* and *Acaryochloris* (28, 29). However, no CYP97 family homologs could be identified in any cyanobacterial databases, including *Prochlorococcus* and *Acaryochloris* (data not shown), which suggests that the acquisition of  $\epsilon$ -hydroxylase activity must have occurred sometime between the evolution of  $\alpha$ -carotene-containing cyanobacteria and the evolution of lutein-containing green algae.

$\epsilon$ -Hydroxylase is a member of the cytochrome P450 family. Plant cytochrome P450s are generally divided into the A type, which is highly conserved and specific to plants, and the non-A type, which is more divergent and similar to nonplant cytochrome P450s (20). Previous phylogenetic analysis has shown that the CYP97 family (which includes the  $\epsilon$ -hydroxylase) belongs to the non-A-type clade and is related most closely to the CYP86 and CYP94 families, both of which use fatty acids as substrates (30). Carotenoids and fatty acids have similar structures and solubilities, and it is conceivable that the  $\epsilon$ -hydroxylase evolved from cytochrome P450-type fatty acid hydroxylases. This would be analogous to the nonheme diiron carotenoid  $\beta$ -hydroxylases that have consensus iron-binding histidine motifs shared with the membrane fatty acid desaturases (24).

In conclusion, we have identified *LUTI* as a member of the cytochrome P450 monooxygenase family that utilizes a hydroxylation mechanism distinct from that of nonheme diiron  $\beta$ -hydroxylases. Cloning of *LUTI* is fundamental for our understanding of lutein biosynthesis, the overlapping functions of different carotenoid hydroxylases, and the regulation of ring hydroxylations *in vivo*. In addition, isolation of a carotenoid hydroxylase triple-knockout mutant has defined the existence of an additional  $\beta$ -hydroxylase *in vivo*.

The University of Wisconsin *Arabidopsis* T-DNA knockout facility provided mutant screening services. This work was supported by National Science Foundation Grant IBN-0131253.

- Niyogi, K. K. (1999) *Annu. Rev. Plant Physiol. Plant Mol. Biol.* **50**, 333–359.
- Hirschberg, J. (2001) *Curr. Opin. Plant Biol.* **4**, 210–218.
- Walton, T. J., Britton, G. & Goodwin, T. W. (1969) *Biochem. J.* **112**, 383–385.
- Milborrow, B. V., Swift, I. E. & Netting, A. G. (1982) *Phytochemistry* **21**, 2853–2857.
- Britton, G. (1998) in *Carotenoids: Biosynthesis and Metabolism*, eds. Britton, G., Liaaen-Jensen, S. & Pfander, H. (Birkhäuser, Basel), Vol. 3, pp. 13–147.
- Cunningham, F. X., Jr., & Gantt, E. (1998) *Annu. Rev. Plant Physiol. Plant Mol. Biol.* **49**, 557–583.
- Shanklin, J., Whittle, E. & Fox, B. G. (1994) *Biochemistry* **33**, 12787–12794.
- Bouvier, F., Keller, Y., d'Harlingue, A. & Camara, B. (1998) *Biochim. Biophys. Acta* **1391**, 320–328.
- Sun, Z., Gantt, E. & Cunningham, F. X. (1996) *J. Biol. Chem.* **271**, 24349–24352.
- Tian, L. & DellaPenna, D. (2001) *Plant Mol. Biol.* **47**, 379–388.
- Pogson, B., McDonald, K. A., Truong, M., Britton, G. & DellaPenna, D. (1996) *Plant Cell* **8**, 1627–1639.
- Tian, L., Magallanes-Lundback, M., Musetti, V. & DellaPenna, D. (2003) *Plant Cell* **15**, 1320–1332.
- Meyer, K., Benning, G. & Grill, E. (1996) in *Genome Mapping in Plants*, ed. Peterson, A. G. (Landes Bioscience, Austin, TX), pp. 137–154.
- Gleave, A. P. (1992) *Plant Mol. Biol.* **20**, 1203–1207.
- Clough, S. J. & Bent, A. F. (1998) *Plant J.* **16**, 735–743.
- Livak, K. J. (1997) *User Bulletin No. 2: ABI PRISM 7700 Sequence Detection System* (PE Applied Biosystems, Foster City, CA), pp. 11–15.
- Thompson, J. D., Gibson, T. J., Plewniak, F., Jeanmougin, F. & Higgins, D. G. (1997) *Nucleic Acids Res.* **24**, 4876–4882.
- Saitou, N. & Nei, M. (1987) *Mol. Biol. Evol.* **4**, 406–425.
- Kumar, S., Tamura, K., Jakobsen, I. B. & Nei, M. (2001) *Bioinformatics* **17**, 1244–1245.
- Chapple, C. (1998) *Annu. Rev. Plant Physiol. Plant Mol. Biol.* **49**, 311–343.
- Schuler, M. A. & Werck-Reichhart, D. (2003) *Annu. Rev. Plant Biol.* **54**, 629–667.
- Berkowitz, J., Ellison, G. B. & Gutman, D. (1994) *J. Phys. Chem.* **98**, 2744–2765.
- Ortiz de Montellano, P. R. (1995) *Drug Metab. Dispos.* **23**, 1181–1187.
- Shanklin, J. & Cahoon, E. B. (1998) *Annu. Rev. Plant Physiol. Plant Mol. Biol.* **49**, 611–641.
- Sono, M., Roach, M. P., Coulter, E. D. & Dawson, J. H. (1996) *Chem. Rev. (Washington, D.C.)* **96**, 2841–2887.
- Yoshizawa, K. (2000) *J. Inorg. Chem.* **78**, 23–34.
- Johnson, E. A. & Schroeder, W. A. (1995) *Adv. Biochem. Eng. Biotechnol.* **53**, 119–178.
- Hess, W. R., Rocap, G., Ting, C. S., Larimer, F., Stilwagen, S., Lamerdin, J. & Chisholm, S. W. (2001) *Photosynth. Res.* **70**, 53–71.
- Miyashita, H., Adachi, K., Kurano, N., Ikemoto, H., Chihara, M. & Miyachi, S. (1997) *Plant Cell Physiol.* **38**, 274–281.
- Paquette, S. M., Bak, S. & Feyereisen, R. (2000) *DNA Cell Biol.* **19**, 307–317.